Sensor and Simulation Notes

Note 416

5 January 1998

Minimizing Dispersion in a TEM Waveguide Bend by a Layered Approximation of a Graded Dielectric Material

W. Scott Bigelow
Everett G. Farr
Farr Research, Inc.

Abstract

Waveguide bends pose a problem for high-voltage ultra-wideband (UWB) systems or for any transmission-line system with low-loss/fast-risetime requirements, since only a straight section of conventional transmission line can support the pure TEM mode necessary to preserve the risetime of a transmitted pulse. Here we consider alternative concepts for compensation of waveguide bends. One concept, a layered approximation of a graded dielectric strip line bend, is built and tested. By reducing the dispersion of a transmitted voltage step, this strip line bend demonstrates the principle of compensation of a waveguide bend by a graded dielectric lens.

1. Introduction

Bends in waveguides pose a problem for high-voltage ultra-wideband (UWB) systems or for any transmission line system with low-loss/fast-risetime requirements. The difficulty arises because only a straight section of conventional transmission line can support the pure TEM mode necessary to preserve the risetime of a transmitted pulse. When there is a bend in the waveguide, especially when the cross-section of the waveguide is large (as it typically must be for high-voltage or low-loss systems), the transmitted signal has a slower risetime than the incident signal. This can severely limit the system bandwidth.

In several papers belonging to this series of notes [1, 2, 3, 4, 5, and 6], Dr. Carl E. Baum describes a new technology which addresses this problem. Specifically, one can embed a waveguide bend within a purely dielectric lens characterized by an inhomogeneous, frequency-independent, isotropic permittivity. Since a properly designed bend employing such a lens will support true TEM waves, even an electrically large bend can be implemented with no dispersion. Use of such bends would permit more compact and convenient designs of high-voltage UWB or low-loss systems.

Although waveguide structures employing lens materials having the required inhomogeneous permittivity profile are easily conceptualized, constructing them is more problematic. Fortunately, an approximation based on graded layers of dielectric materials of various uniform permittivities should be adequate for a pulse with a risetime comparable to or longer than the greatest difference in signal transit times through the bend for any two layers. Use of such graded layers of dielectric materials would permit economical commercial fabrication of electrically large, low-dispersion waveguide bends.

In this note, we describe the design and performance of a strip transmission line with a 90-degree bend embedded in a lens consisting of graded layers of dielectric materials. First, we provide an overview of the graded dielectric lens concept, and we survey the implementation alternatives considered. Then, we summarize our hardware implementation of a graded dielectric strip line bend. Although a leaky structure, such as a curved strip line, cannot be expected to perform as well, for example, as a coaxial line, it is easier to build than a coaxial line; and it serves to demonstrate the principle of compensation of a bend by use of a graded dielectric lens.

2. Overview of the Graded Dielectric Lens Concept

Consider the waveguide bend shown in Figure 1, which consists of a strip transmission line above a ground plane, all in air. The straight sections of the waveguide are known to support the non-dispersive propagation of a pure TEM wave, provided that the conductors are perfectly conducting—in practice, there is some dispersion due to finite conductivity. However, the curved section cannot support a pure TEM wave. This is readily apparent, since rays entering the bend at its outer edge must travel farther than those entering at the inside edge. As a result, they lag behind those at the inside edge. What is needed is a way to equalize the transit times for all rays propagating through the bend.

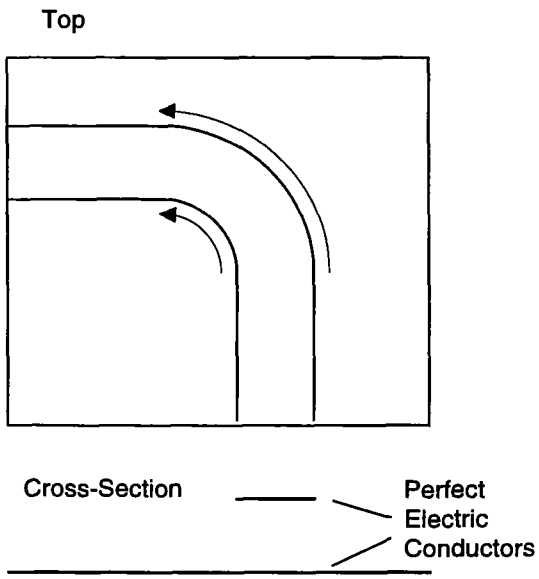

Figure 1. Waveguide bend, showing why a wave becomes dispersed at a bend. A ray on the outside curve travels farther than one on the inside curve.

For a purely dielectric (non-magnetic) material, transit times through a bend are equalized if the product of the radius of curvature and the square root of the permittivity is constant. Thus, a very simple method of equalizing transit times is to embed the strip line in a material whose permittivity varies inversely as the square of the radius. This is expressed as [2]

$$\varepsilon(\Psi) = \varepsilon_o \times \left(\frac{\Psi_{max}}{\Psi}\right)^2 \tag{1}$$

where Ψ is the cylindrical radius of curvature in the usual (Ψ, ϕ, z) cylindrical coordinate system, and ε_o is the permittivity of free space. Here, it is assumed that at some outer radius, Ψ_{max}, the fields no longer contribute significantly; and the permittivity reaches a minimum, in this case ε_o. This is shown conceptually below in Figure 2.

3. Implementation of a Compensated Waveguide Bend

We considered several alternative hardware implementations of non-dispersive waveguide bends. Ultimately, we selected a strip line bend embedded within graded dielectric layers machined from sheets of low-loss, uniform-permittivity plastic materials. This design represented a compromise between modeling fidelity and ease of construction. We first review the other candidate approaches we considered. Then we discuss the design and testing of the graded dielectric strip line bend.

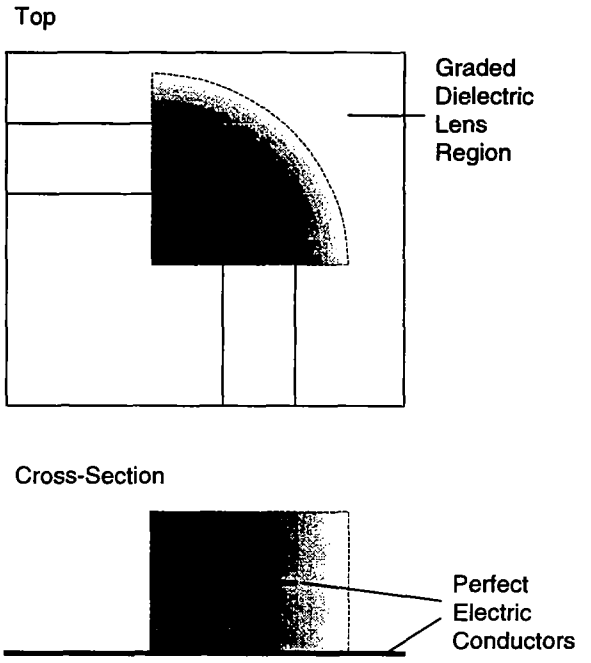

Figure 2. Compensation of a waveguide bend by a graded dielectric material. Within the bend, the permittivity varies inversely as the square of the radius of curvature.

3.1 Approaches Considered

The first approach considered was to build cylindrical layers having differing permittivities by using combinations of epoxy and titanium dioxide powder. Higher concentrations of titanium dioxide provide higher permittivities. In this approach, one would add successive layers to the inside of a cylinder, with each layer having a slightly higher permittivity than its predecessor. One would make each layer uniform by spinning the cylinder at a high angular speed, as indicated by Figure 3. A fourth of the resulting cylindrical shell of graded dielectric material could be sectioned and used to compensate a 90-degree strip line bend. A similar approach might be useful for building up layers inside a coaxial bend, which is just a section of a torus of circular cross-section. One can anticipate, however, a number of difficulties in working with the mixtures of epoxy and titanium dioxide. A well-controlled process would have to be used to control the blending of the mixtures in order to achieve

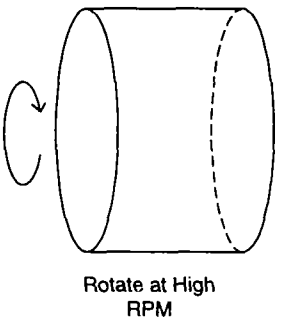

Figure 3. Graded dielectric fabrication technique using successive layers of epoxy loaded with titanium dioxide.

reproducibility of the permittivity for each radius of curvature. A similarly well-controlled process would be needed to deposit and cure each layer. While these obstacles could likely be overcome in a production-scale facility, they would pose unnecessary difficulties for an initial proof-of-principle hardware demonstration.

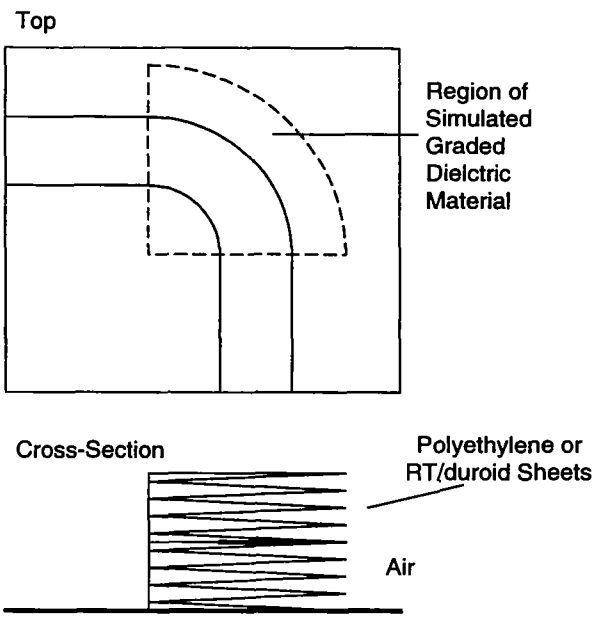

Figure 4. One method of building a simulated graded dielectric material, using a stack of uniform-permittivity wedges in a saw-tooth pattern.

Another option considered was to build the dielectric material from a single uniform material by use of cylindrical sheets arranged to form a saw-tooth pattern. This would simulate a graded dielectric material. A diagram of this idea is shown in Figure 4. One could use a printed circuit board laminate for the dielectric sheets. The thickness of the sheets could be about 0.76 mm, which is thick enough so that each sheet would be self-supporting. A further simplification of this approach would be the use of a single cylindrical wedge, as shown in Figure 5. The single wedge could be readily cut under computer control, and its use would obviate the complex assembly process required for a stack of dielectric sheets.

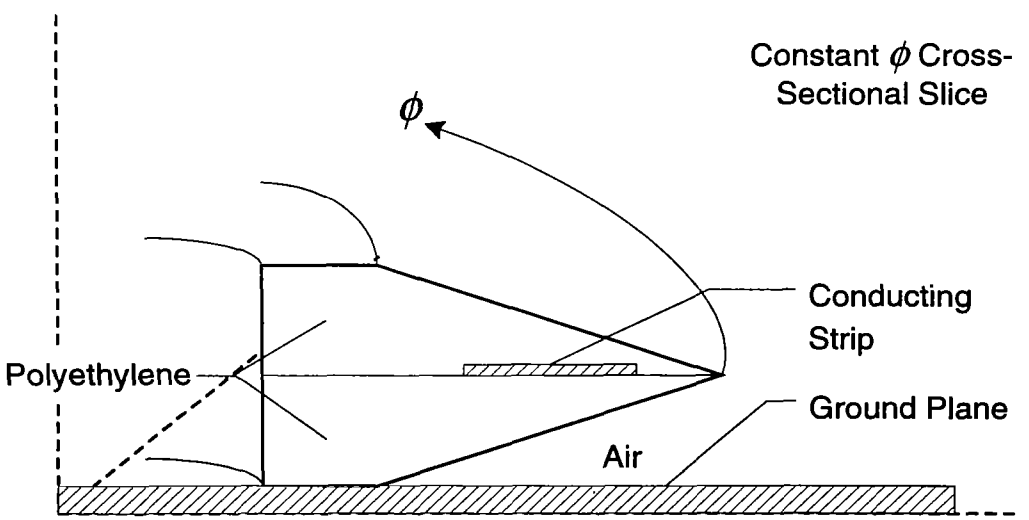

Figure 5. Strip line bend partially filled with dielectric in the form of a single cylindrical wedge.

A disadvantage of these uniform material configurations is that the resulting effective permittivity is anisotropic. In other words, at a given point there is a different permittivity for electric fields polarized horizontally and vertically. This is potentially a problem, because the theory assumes an isotropic material.

Consideration of parallel plate capacitors partially filled with a uniform dielectric serves to clarify the anisotropic nature of the effective permittivity. For the case of the electric field vector, **E**, perpendicular ($\perp$) to the dielectric interface, as in Figure 6, the filled and unfilled portions of the gap appear as two capacitors in series. For the total capacitance we have

$$C_{\perp} = \frac{1}{1+\left(\varepsilon_r^{-1}-1\right)f}\frac{\varepsilon_0 A}{d} \qquad (2)$$

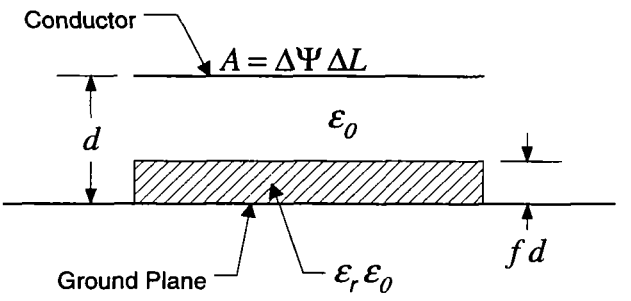

Figure 6. Partially filled parallel plate capacitor with electric field perpendicular to the dielectric-air interface.

where ε_r is the relative permittivity of the fill material, f is the fraction of the gap, d, which is filled. This expression defines the effective relative permittivity for **E** perpendicular to the dielectric interface as

$$\varepsilon_{\perp} = \frac{1}{1+\left(\varepsilon_r^{-1}-1\right)f} \qquad (3)$$

If, on the other hand, the dielectric-filled fraction extends all the way across the gap, d, but does not fill completely the $\Delta\Psi$ width of the capacitor, then **E** is parallel to the dielectric-air interface, and the filled and unfilled regions are like two capacitors in parallel ($\parallel$). Thus, we have

$$C_{\parallel} = \left[1+(\varepsilon_r-1)f\right]\frac{\varepsilon_0 A}{d} \qquad (4)$$

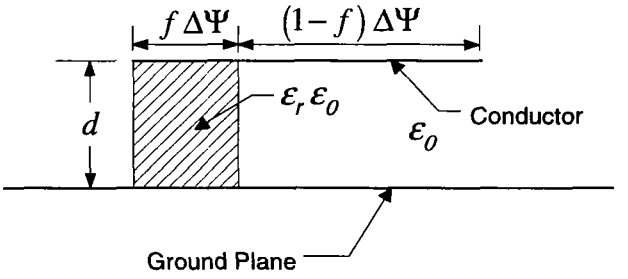

Figure 7. Partially filled parallel plate capacitor with electric field parallel to the dielectric-air interface.

This defines the effective relative permittivity for **E** parallel to the dielectric interface as

$$\varepsilon_{\|} = 1 + (\varepsilon_r - 1) f \tag{5}$$

The following figure uses the quantity, $r_\varepsilon = 1 - \varepsilon_\perp / \varepsilon_{\|}$, as a measure of the anisotropy in the effective relative permittivity. The anisotropy increases with the permittivity of the fill material and is largest for a half-filled capacitor.

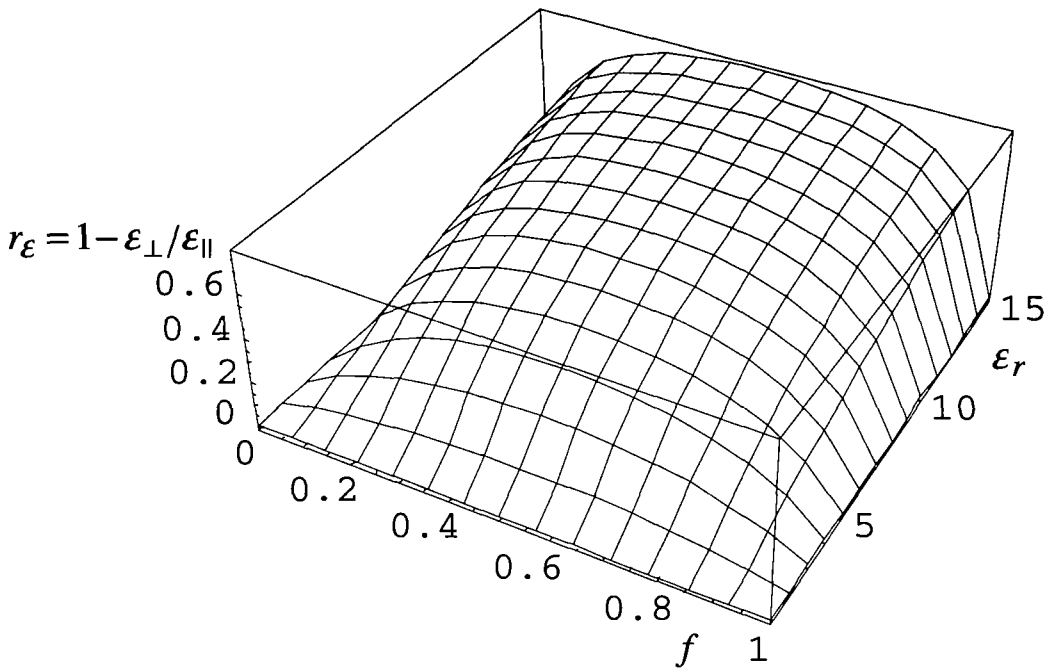

Figure 8. Anisotropy of the effective relative permittivity for a parallel plate capacitor partially filled with a uniform dielectric material.

To design a waveguide bend compensated by a partial filling of dielectric material, we need to establish the fill fraction required to produce an effective permittivity which varies inversely with the square of the radius of curvature. The preceding expressions for $\varepsilon_{\|}$ and $\varepsilon_\perp$ can be inverted to obtain fill-fraction expressions for parallel and perpendicular electric fields as

$$f_\perp = \frac{1 - \varepsilon_{r,eff}^{-1}}{1 - \varepsilon_r^{-1}} \quad \text{and} \quad f_{\|} = \frac{\varepsilon_{r,eff} - 1}{\varepsilon_r - 1} \tag{6}$$

where, from (1), we have $\varepsilon_{r,eff} = (\Psi_{\max} / \Psi)^2$.

In Figure 9, we present the result of a calculation in which a strip line was modeled as a parallel plate capacitor partially filled with a uniform dielectric material with $\varepsilon_r = 2.2$. Although the geometry of the fill material is not specified, the figure shows the required fill fraction as a function of radial position for both parallel and perpendicular orientations of the electric field relative to the dielectric-air interfaces. This result illustrates the problem posed by an anisotropic effective permittivity. It is not possible to specify a unique fill fraction for each radius of curvature, as the appropriate fill fraction depends on the local orientation of the electric field.

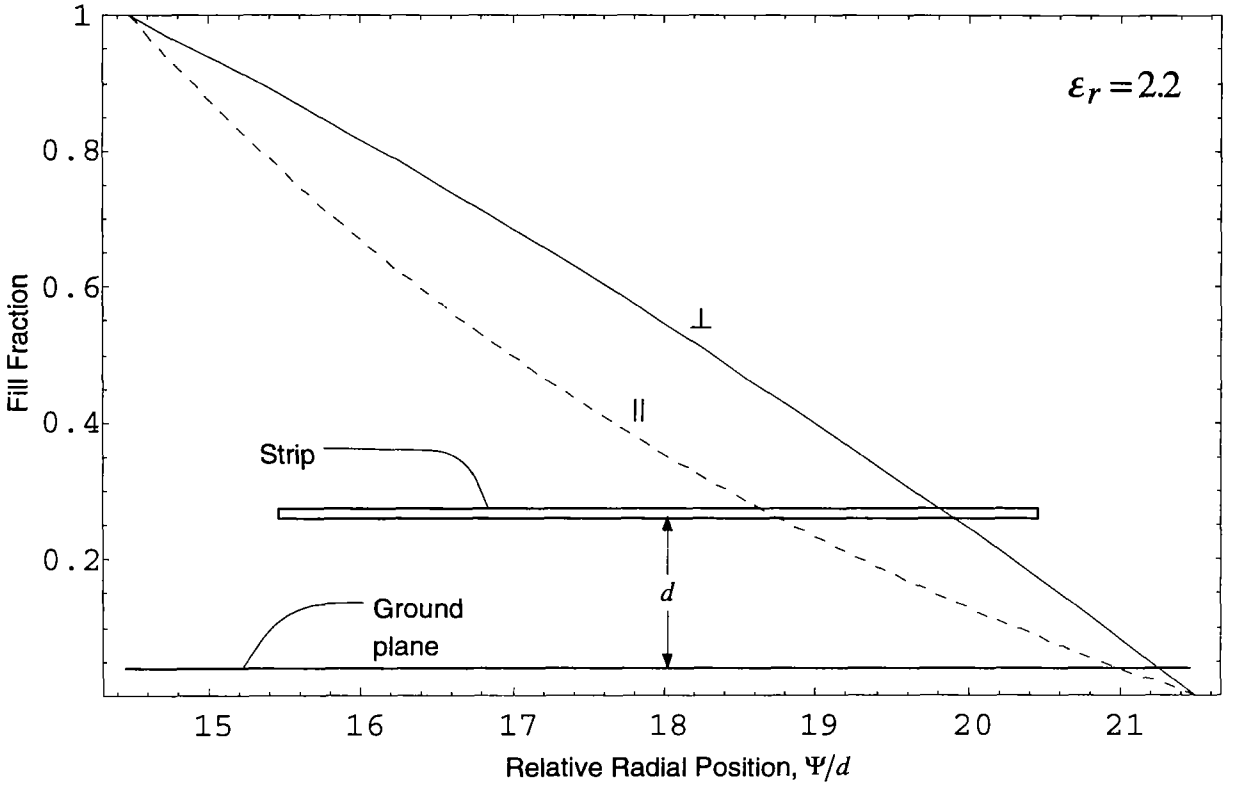

Figure 9. Dielectric fill fraction, as a function of radial position, required to produce an effective relative permittivity that varies inversely as the square of radial position. The two curves correspond to the electric field vector aligned either parallel (||) or perpendicular (⊥) to the dielectric-air interfaces. The calculation assumed a strip line of width $5d$, located a distance, d, above a ground plane. Fringe fields were neglected. The relative permittivity of the fill material is 2.2.

Another bend compensation approach we considered was to embed wedges of high-permittivity materials in a direction perpendicular to the direction of propagation. A sketch of this concept is shown in Figure 10. Because of the differing radii of curvature, there is relatively more high-permittivity material along the inner curve than along the outer curve. By adjusting the number and thickness of the wedges, the profile of the effective permittivity may be tailored. Here, there is no difficulty with anisotropy, since the fields are parallel to the dielectric-air interfaces. However, the granularity of the wedges must be sufficiently fine that the wedge transit times remain short compared to the risetime. Also, multiple reflections from the wedge surfaces could pose a problem. As a result, this approach could be more useful with an E-plane bend, where reflections might be minimized by arranging the dielectric surfaces at Brewster's angle relative to the electric field vector.

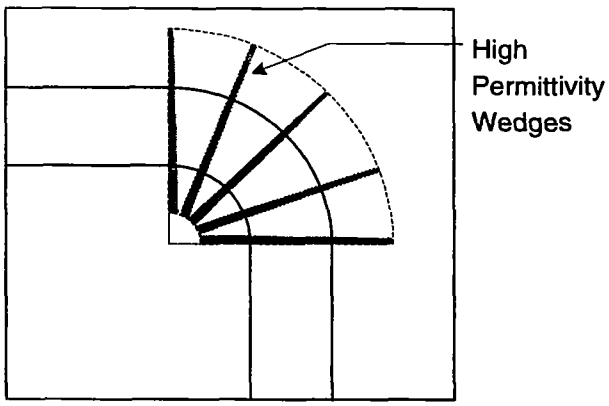

Figure 10. Use of high-permittivity wedges oriented radially.

3.2 Design and Testing of the Graded Dielectric Strip Line Bend

We now describe the design and testing of a layered approximation of a graded dielectric material as a compensating lens for a strip line bend. Our test fixture layout is depicted in Figure 11. With the straight section in place, measurements were made between Port 1 and Port 2. With the curved section, measurements were made between Port 1 and Port 3. The curved conducting strip was used both with and without the graded dielectric lens.

Although we originally intended to maintain approximately 50 ohms impedance with the dielectric lens in place, this would have required a very narrow strip width within the bend region and almost no resolution in permittivity across the strip. We decided, instead, to maintain a constant strip width, corresponding to approximately 50 ohms in air, as shown in the figure. With the lens in place, this choice led to large impedance discontinuities at the entrance and exit of the bend. Nevertheless, this design afforded a broader permittivity range across the width of the strip, and we were convinced that such a range would be necessary to demonstrate compensation of the bend. Figure 12 compares permittivity and location of each dielectric layer with the ideal permittivity profile for the graded bend. Details of the dielectric material layout in the bend region are shown in Figure 13.

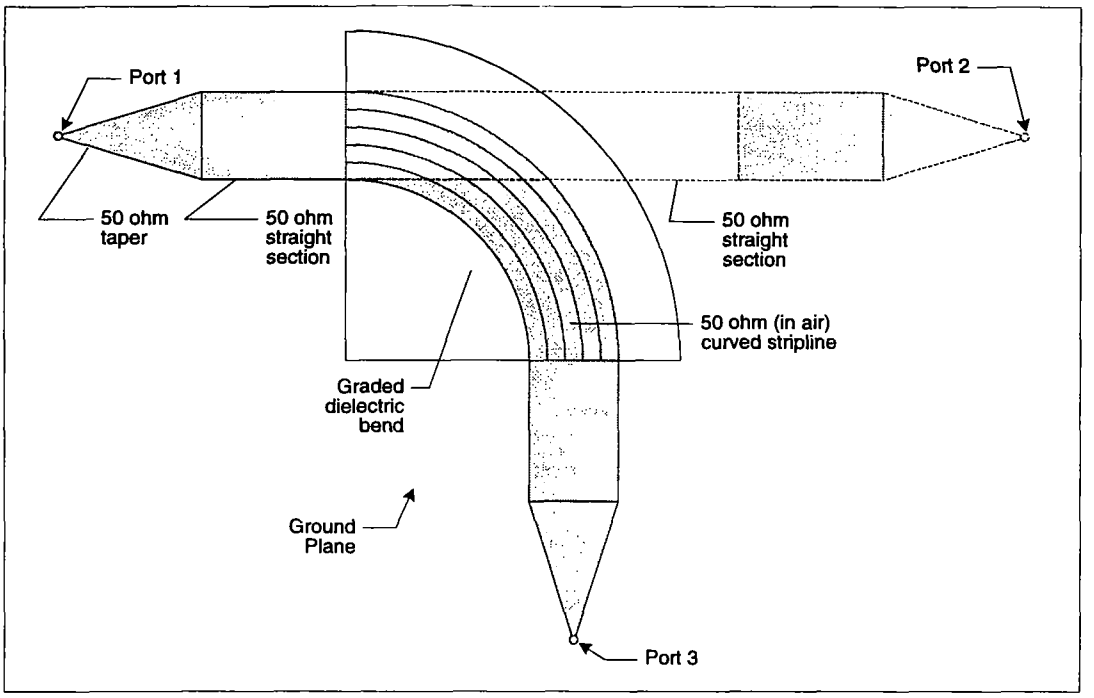

Figure 11. Strip line test fixture layout.

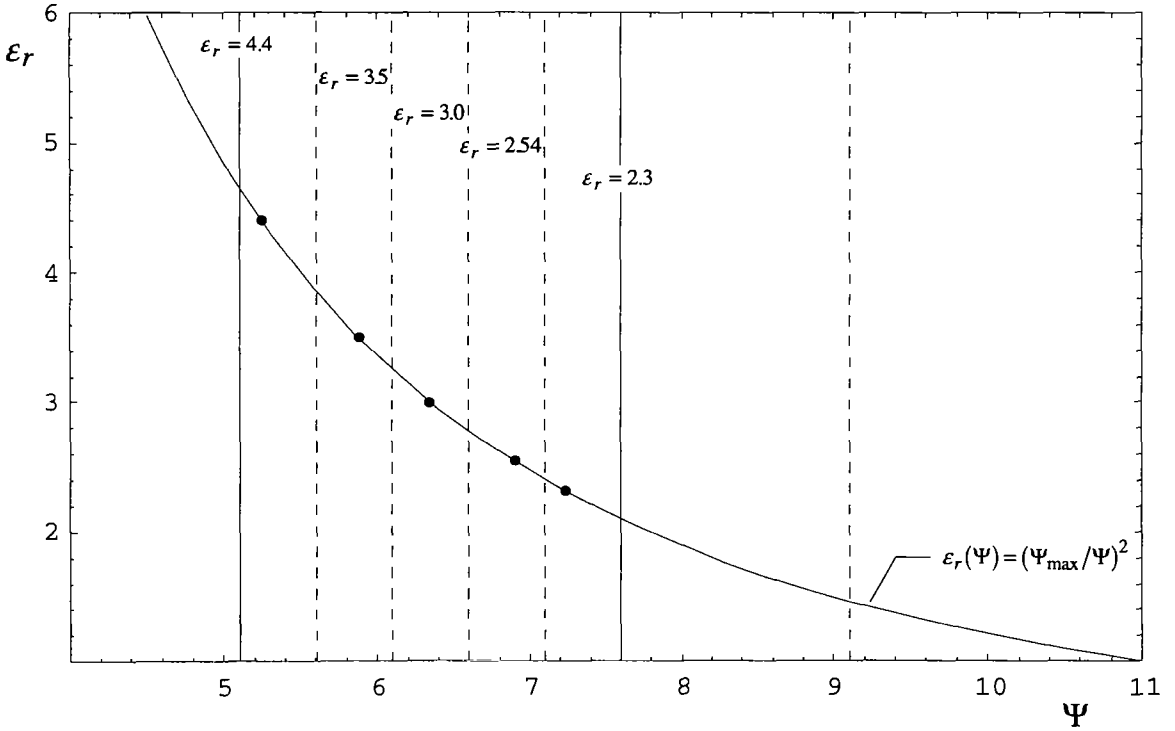

Figure 12. Five-layer approximation to an ideal permittivity profile for a graded dielectric bend. The solid vertical lines indicate the edges of the conducting strip. The dashed lines indicate the boundaries between uniform dielectric layers.

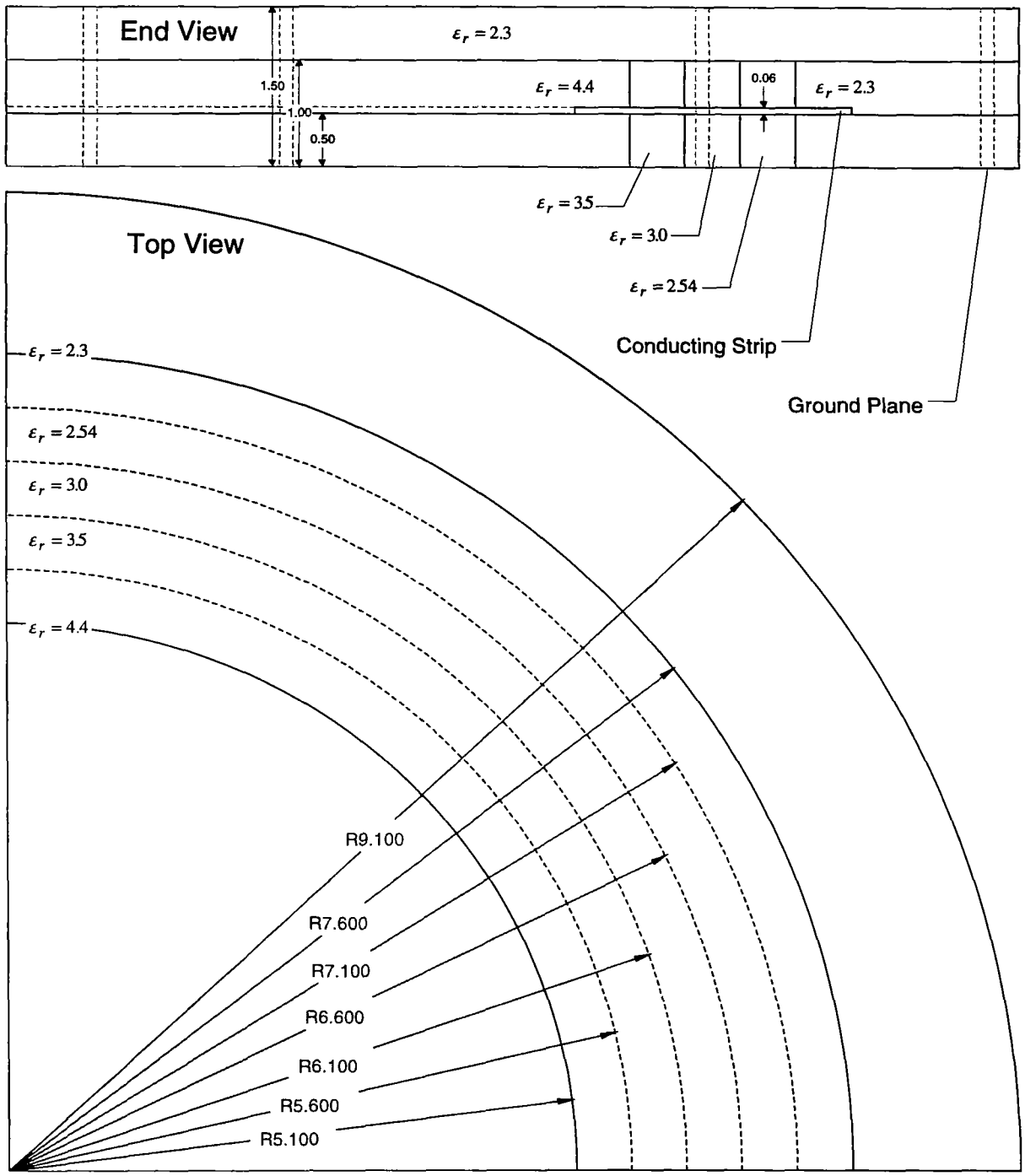

Figure 13. Five-layer graded dielectric bend assembly. Straight sections at the entrance and exit of the bend are not shown. The conducting strip is 1.27 cm (0.5 in.) above the ground plane. Its width is a constant 6.35 cm (2.5 in.) in both straight and curved regions. Within the strip boundaries, the relative permittivities approximate an inverse square law relationship with the radius of curvature. The relative permittivity, ε_r, is assumed to be 1.0 at a radius of 27.94 cm (11.0 in.).

To find the characteristic impedance of the graded dielectric structure, one solves a two-dimensional equation in cylindrical coordinates, in a plane of constant azimuth, ϕ. In terms of the electric potential, $V(\Psi,z)$, the equation to be solved is [6 (7.9)]

$$\Psi \frac{\partial}{\partial \Psi}\left(\frac{1}{\Psi}\frac{\partial V}{\partial \Psi}\right) + \frac{\partial^2 V}{\partial z^2} = 0 \tag{7}$$

where the boundary conditions are $V = V_0$ on the conducting strip and $V = 0$ on the ground plane. To maintain a constant wavefront velocity around the bend, the permittivity, ε, must vary inversely as the square of the radius in the bend region, as specified previously in (1). In principle, one can then calculate the charge per unit angle (ϕ) on the center conductor. From the charge per unit angle and the angular wave propagation speed around the bend (in radians per second), the current may be obtained. With the voltage and current calculated, the characteristic impedance is their ratio.

As a first approximation, we decided to solve an easier problem. Specifically, we assumed that the change in azimuth through the bend could be ignored—a straight strip approximation. This permitted us to treat Ψ and z as Cartesian coordinates, and reduced our problem to solving Laplace's equation,

$$\nabla \bullet (\varepsilon_i \nabla V) = 0 \tag{8}$$

over a rectangular (Ψ, z) domain consisting of piecewise-constant-permittivity sub-domains. The permittivity, $\varepsilon_i = \varepsilon_{r,i}\,\varepsilon_0$, is uniform within each sub-domain; and the voltage is given by $V = V_0$ on the strip, and by $V = 0$ on the ground plane. This approximation is justified later by the solution of simple canonical problems, and by the results of time-domain reflectometry (TDR) measurements.

We solved (8) by the finite element method. Then, as described by Silvester & Ferrari [7], we exploited the fact that the finite element method provides an estimate of the stored field energy as

$$W = \frac{1}{2}\int_{\Omega} \varepsilon \mathbf{E}^2 d\Omega \approx \frac{1}{2}\mathbf{U}^{\mathrm{T}}\mathbf{S}\mathbf{U} \tag{9}$$

where $\mathbf{S}$ is the assembled finite element matrix; and the vector $\mathbf{U}$, defined on the nodes of the finite element mesh, is the finite element approximation to V. The capacitance can be estimated

from the fact that the stored energy is also given by

$$W = \frac{1}{2} C V_0^2 \tag{10}$$

Noting that the wave velocity, v, is given by $v = 1/\sqrt{\mu\varepsilon}$, we get the characteristic impedance from $Z_c = (vC)^{-1}$, by combining (9) and (10), as

$$Z_c = \frac{\sqrt{\mu_0 \varepsilon_0 \varepsilon_{r,eff}}\, V_0^2}{\mathbf{U}^T \mathbf{S} \mathbf{U}} = \frac{Z_0 \varepsilon_0 \sqrt{\varepsilon_{r,eff}}\, V_0^2}{\mathbf{U}^T \mathbf{S} \mathbf{U}} \tag{11}$$

where we assume a pure dielectric ($\mu = \mu_0$), and we interpret $\varepsilon_{r,eff}$ as an effective relative permittivity for the dielectric layers within the width of the conducting strip. We assume that the effective permittivity is simply the arithmetic average of the permittivity of each layer. This is equivalent to treating the strip and graded dielectric layers as a parallel array of capacitors. For an electric field predominantly parallel to the dielectric layer interfaces, this is a valid approach.

In our finite element model, we defined sub-domains, as shown in Figure 14, for each dielectric material in the model space. With $\varepsilon_{r,eff} = 3.1$, the method produces a characteristic impedance of 28 ohms, in agreement with a TDR measurement of the bend (Figure 15).

As a check on these results, we modeled the bend using three different analytic approximations. A closed-form analytic result for a pair of infinitesimally thin plates embedded in a uniform dielectric (a straight strip approximation which includes the fringe field contribution) yields a characteristic impedance of 98 ohms in air (see, for example, [8, 9, 10, and 11]). With an effective relative permittivity of 3.1 (the average relative permittivity for the materials used in the bend), this is equivalent to 28 ohms for a single plate over a ground plane. For the same one-half parallel plate transmission line, in which both plate thickness and fringe fields are neglected, the calculated characteristic impedance,

$$Z_c = Z_0 \left(\Delta z / \Delta \Psi\right) / \sqrt{\varepsilon_{r,eff}} \tag{12}$$

is 43 ohms. An approach described by Baum [2] produces a closed-form solution for a continuously graded H-plane bend, subject to the assumption that fringe fields can be neglected. For a bend equivalent to our graded bend (see Appendix A), that method also leads to a value of 43 ohms.

Since both graded bend and parallel plate results (neglecting fringe fields) are in agreement, we have some confidence that a straight strip approximation to the bend is a good approximation, as is the use of the average of the relative permittivities of the materials within the strip width. In turn, these conclusions give us confidence that the 28 ohm straight strip results, produced by both the analytic and the finite element numerical methods, represent good approximations for the graded bend, when fringe fields are considered. Thus, both measurement and numerical analysis agree that 28 ohms is a good estimate of the characteristic impedance of the graded bend.

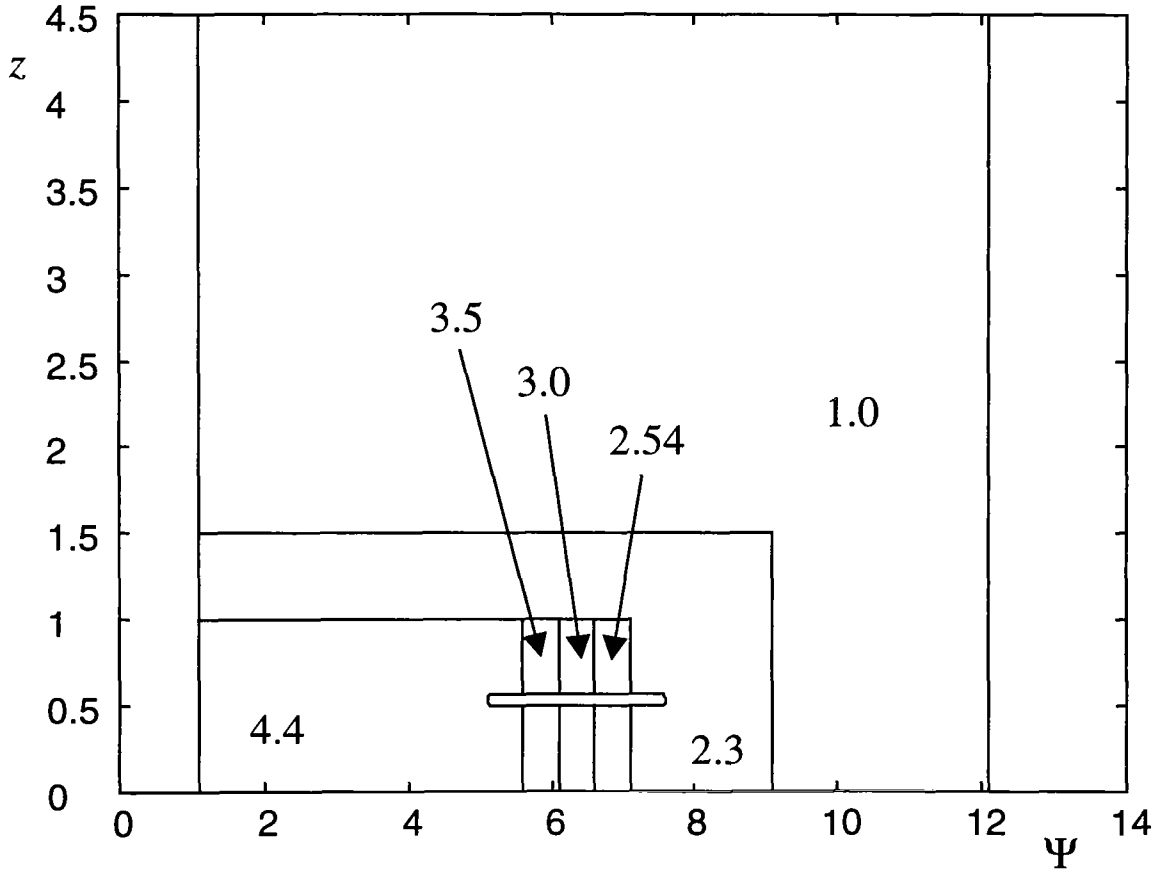

Figure 14. Geometry for finite element model of the five-layer graded dielectric bend. Relative permittivities used for the sub-domains are indicated. (Note that the vertical scale has been expanded for clarity. Units for both axes are inches.)

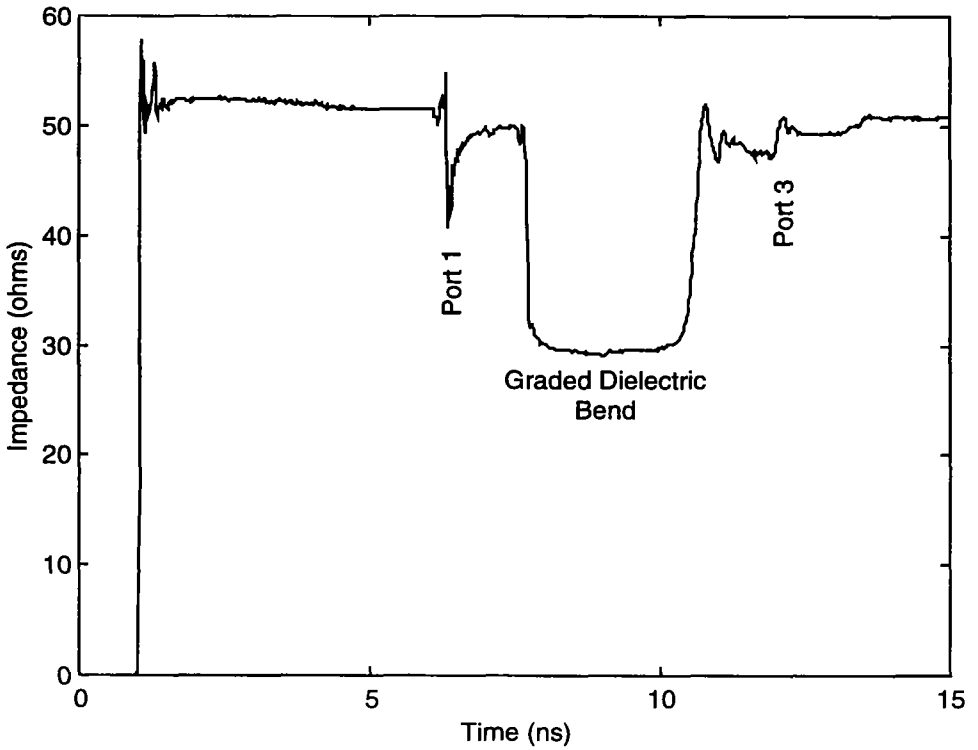

Figure 15. TDR measurement of a strip line with a 90-degree bend embedded within a five-layer approximation of a graded dielectric material. Within the bend region, the impedance is approximately 28 ohms.

In Figure 16, transmission of a voltage step pulse through the straight, air-filled strip line section (between Port 1 and Port 2), is compared with transmission of the same pulse through the curved section (between Port 1 and Port 3), both air-filled and compensated by the five-layer graded dielectric lens. The data for the compensated bend were normalized to remove the 8% reflection loss that results from traversing the two dielectric-air interfaces, where the impedance transitions between 50 and 28 ohms. The fall time of the pulse at the source (not shown) was 32 ps. Transmission through the straight strip line section (and the feed sections) degraded the fall time to 75 ps. This is the best we can expect for a perfectly compensated bend. The air-filled bend degraded the fall time to 255 ps. The graded dielectric layers improved the transmission through the bend, reducing the fall time to 185 ps. However, this is still more than twice the fall time observed with the straight strip line section.

The primary causes of the imperfect compensation of the bend appear to lie in the finite thickness of the dielectric layers, and in the permittivities of the materials filling the fringe field

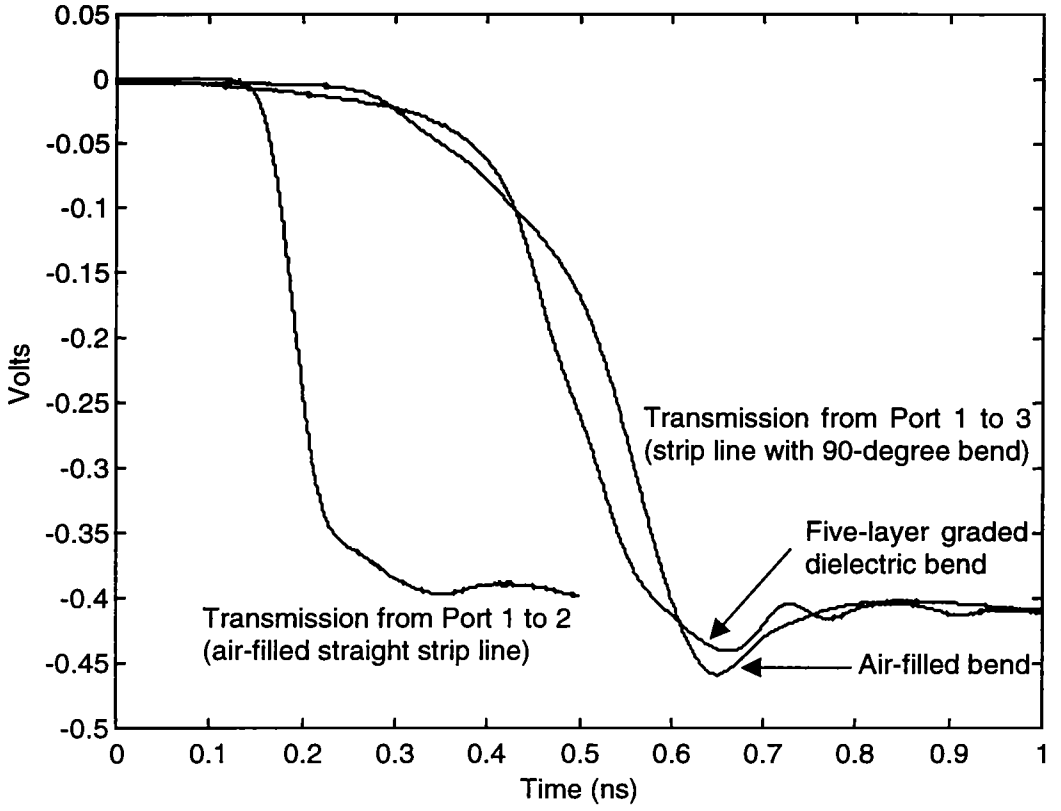

Figure 16. Transmission of a voltage step by straight and curved strip lines. The fall time for the straight line is approximately 75 ps. With the air-filled, 90-degree bend, the fall time increases to approximately 255 ps. For the same bend with a five-layer radially graded dielectric lens, the fall time is reduced to approximately 185 ps. The data are normalized to correct for reflection losses at the dielectric-air interfaces.

regions on each edge of the strip. The difference in transit time around the bend at the strip edges is 330 ps for the air bend; for the lensed bend, the difference is 110 ps. However, the transit time difference for the lensed bend climbs to 350 ps when fringe regions 1.27 cm on each side of the strip are considered. If we calculate the transit times along each dielectric layer interface, we find that the differences in transit times within the dielectric layers immediately adjacent to each interface range from a low of 74 ps to a high of 170 ps. All these differences in transit time combine to stretch the transmitted pulse.

Other contributors to the observed imperfect compensation of the bend are pulse distortion resulting from the impedance discontinuities at the entrance and exit of the bend, and dispersive attenuation of the transmitted pulse.

4. Concluding Remarks

Although the five-layer graded dielectric bend substantially improved the transmission of a stepped voltage pulse through the curved section of our strip line test fixture, the fall time of the pulse was still more than twice that observed for propagation through an equivalent straight section. Several features of the design may contribute to this situation. Among the significant design issues are: (1) the accuracy of the layered approximation to the ideal continuously graded bend, (2) pulse distortion at the impedance discontinuities at the entrance and exit of the bend, and (3) dispersive attenuation of the pulse.

Inaccuracies in the layered approximation of the graded dielectric bend led to significant differences in pulse transit time through the bend. The transit time differences introduced by the fringe field regions were especially large. Thus, variations in transit time through the bend appear to have been major contributors to the observed pulse stretching.

Although the impedance discontinuities at the entrance and exit of the bend led to reflection losses on the order of 8%, no other negative impacts on the transmitted pulse are apparent. Since the reflective losses appear to account for the degradation in the magnitude of the transmitted pulse, attenuation by the dielectric material does not appear to be a significant issue.

In the future, we plan to design a graded coaxial transmission line bend. This should be almost as easy to fabricate as the leaky strip line bend, and fortunately, fringe fields will not be an issue for a coaxial geometry. We anticipate that a finely graded coaxial line will be capable of extremely low-dispersion transmission. Moreover, by eliminating dielectric-air interfaces, we will be able to reduce reflective losses.

Acknowledgments

We would like to thank Mr. William B. Prather of Phillips Laboratory for funding this work. We are similarly indebted to Dr. Carl E. Baum, also of Phillips Laboratory, for his pioneering theoretical work in this area and for his many helpful discussions that contributed to this effort.

Appendix A. Impedance of a Graded Dielectric H-plane Bend Where Fringe Fields are Neglected

In [2], Dr. Baum develops an analytic solution for the impedance of an H-plane bend filled with a purely dielectric material whose permittivity varies continuously with the radius of curvature. That solution assumes fringe fields can be neglected, so that the only electric field component is directed normally to the conductor surfaces. Although this is not a good assumption for our geometry, we use this model to obtain an upper bound on the impedance of our graded dielectric bend.

From [2 (3.7), (3.8), and (3.12)], we have

$$\begin{aligned} \varepsilon &= \left(\frac{\Psi}{\Psi_{\max}}\right)^2 \varepsilon_{\min} \\ Z_o' &= \sqrt{\mu/\varepsilon_{\min}} \\ Z_c &= Z_o' \frac{\Delta u_1}{\Delta u_2} \end{aligned} \tag{13}$$

where Z_o' is the formal wave impedance, and we choose $\mu = \mu_o$ and $\varepsilon_{\min} = \varepsilon_o$, so that $Z_o' = Z_o = 376.727$ ohms. Now, for the H-plane bend with perfectly conducting boundaries on planes of constant z, separated by a distance small in comparison to their Ψ extent, the electric field is entirely in the z-direction, and from [2 (4.1)] we have the relationships

$$\begin{aligned} u_1 &= z \quad \text{and} \\ u_2 &= \Psi_{\max} \log_e(\Psi/\Psi_{\max}) \end{aligned} \tag{14}$$

Now, for our design (Figure 13)

$$\begin{aligned} \Delta u_1 &= \Delta z \quad \text{and} \\ \Delta u_2 &= \Psi_{\max} \log_e(\Psi_2/\Psi_1) \end{aligned} \tag{15}$$

where Δz = 1.27 cm (0.5 in.), $\Psi_{\max}$ = 27.94 cm (11.0 in.), Ψ_2 = 19.30 cm (7.6 in.), and Ψ_1 = 12.95 cm (5.1 in.). Thus, from (13), we have the characteristic impedance, $Z_c = 43$ ohms.

References

1. Baum, Carl E., *Two-Dimensional Inhomogeneous Dielectric Lenses for E-Plane Bends of TEM Waves Guided Between Perfectly Conducting Sheets*, Sensor and Simulation Notes, Note 388, 14 October 1995.

2. Baum, Carl E., *Dielectric Body-of-Revolution Lenses with Azimuthal Propagation*, Sensor and Simulation Notes, Note 393, 9 March 1996.

3. Baum, Carl E., *Dielectric Jackets as Lenses and Application to Generalized Coaxes and Bends in Coaxial Cables*, Sensor and Simulation Notes, Note 394, 23 March 1996.

4. Baum, Carl E., *Azimuthal TEM Waveguides in Dielectric Media*, Sensor and Simulation Notes, Note 397, 31 March 1996.

5. Baum, Carl E., *Discrete and Continuous E-Plane Bends in Parallel-Plate Waveguide*, Sensor and Simulation Notes, Note 399, 1 May 1996.

6. Baum, Carl E., *Use of Generalized Inhomogeneous TEM Plane Waves in Differential Geometric Lens Synthesis*, Sensor and Simulation Notes, Note 405, 5 December 1996.

7. Silvester, P. P. and R. L. Ferrari, *Finite Elements for Electrical Engineers*, 2nd Ed., Cambridge University Press, Cambridge CB2 1RP, 1990, p. 208 et seq.

8. Farr, Everett G., *Optimization of the Feed Impedance of Impulse Radiating Antennas Part II: TEM Horns and Lens IRAs*, Sensor and Simulation Notes, Note 384, November 1995.

9. Farr, Everett G., *Optimizing the Feed Impedance of Impulse Radiating Antennas, Part I, Reflector IRAs*, Sensor and Simulation Notes, Note 354, January 1993.

10. Baum, Carl E., D. V. Giri, and R. D. Gonzalez, *Electromagnetic Field Distribution of the TEM Mode in a Symmetrical Two-Parallel-Plate Transmission Line*, Sensor and Simulation Notes, Note 219, April 1976.

11. Baum, Carl E., *Impedances and Field Distributions for Parallel Plate Transmission Line Simulators*, Sensor and Simulation Notes, Note XXI, June 1966.